RSK2 inactivation cooperates with AXIN1 inactivation or β-catenin activation to promote hepatocarcinogenesis

Samantha Schaeffer, Barkha Gupta, Anna-Line Calatayud, Julien Calderaro, Stefano Caruso, Théo Hirsch, Laura Pelletier, Jessica Zucman-Rossi, Sandra Rebouissou

Journal of Hepatology

RSK2 inactivation cooperates with AXIN1 inactivation or ß-catenin activation to promote hepatocarcinogenesis

--Manuscript Draft--

Manuscript Number:	JHEPAT-D-22-01812R2
Article Type:	Original Article
Section/Category:	Hepatic and Biliary Cancer
Keywords:	hepatocellular carcinoma; RSK2; AXIN1; ß-catenin; mouse models; RAS/MAPK signaling
First Author:	Samantha Schaeffer
Corresponding Author:	Sandra Rebouissou Paris, FRANCE
Order of Authors:	Samantha Schaeffer
	Barkha Gupta
	Anna-Line Calatayud
	Julien Calderaro
	Stefano Caruso
	Théo Hirsch
	Laura Pelletier
	Jessica Zucman-Rossi
	Sandra Rebouissou
Abstract:	Background & Aims: Recurrent somatic mutations of RPS6KA3 gene encoding for the serine/threonine kinase RSK2 were identified in hepatocellular carcinomas (HCC) suggesting its tumor suppressive function. Our goal was to demonstrate the tumor suppressor role of RSK2 in the liver and investigate the functional consequences of its inactivation. Methods: We analyzed a series of 1151 human HCCs for RSK2 mutations and 20 other driver genetic alterations. We then modeled RSK2 inactivation in mice in various mutational contexts recapitulating or not those naturally found in human HCC, using transgenic mice and liver-specific carcinogens. These models were monitored for liver tumor appearance and subjected to phenotypic and transcriptomic analyzes. Functional consequences of RSK2 rescue were also investigated in a human RSK2 deficient HCC cell line. Results: RSK2 inactivating mutations are specific of human HCC and frequently co-occur with AXIN1 inactivating or ß-catenin activating mutations. Modeling of these co-occurrences in mice showed cooperative effect in promoting liver tumors with transcriptomic profiles recapitulating those of human HCCs. By contrast, there was no cooperation in liver tumor induction between RSK2 loss and BRAF activating mutations chemically induced by diethylnitrosamine. In human liver cancer cells, we also showed that RSK2 inactivation confers some dependency to the activation of the RAS/MAPK signaling that can be targeted by MEK inhibitors. Conclusions: Our study newly demonstrated the tumor suppressor role of RSK2 and its specific synergistic effect in hepatocarcinogenesis when its loss of function is specifically combined with AXIN1 inactivation or ß-catenin activation. Furthermore, we identified the RAS/MAPK pathway as a potential therapeutic target for RSK2-inactivated liver tumors.
Response to Reviewers:	

JOURNAL OF HEPATOLOGY

Journal of Hepatology

Revised Submission Checklist

This form must be completed and submitted for all revised manuscripts. Without this form the manuscript will be returned to the corresponding author for completion.

Corresponding Author:	Sandra REBOUISSOU
Manuscript Number:	JHEPAT-D-22-01812

Below, provide the page number(s) or figure legend(s) where the information can be located. Please make sure that all the information requested below is present in the manuscript.

		Completed, or reported on page(s) or figure legend(s):
1)	**Submission**	
a)	Title page: COI, Financial support, Authors' contributions, keywords.	Y
b)	Structured abstract and lay summary	Y
c)	All tables and figures included, numbered correctly, with legends (p value and statistical test)	Y
d)	Supplementary data included in a single, separate word file	Y
e)	A detailed point by point response to reviewers comments and changes highlighted in text	Y
f)	All authors to complete and upload an ICMJE conflict of interest form.	Y
g)	Graphical abstract	Y
2)	**Materials and methods**	
a)	Completed the CTAT form for all reagents and resource to be added to supplementary material	Supp data P2-5
b)	Identify the source and authentication of cell lines	Supp data P2-3
c)	Identify animal species, number of animals used, strain, sex and age.	Supp data P3
d)	For animal studies include a statement of compliance with ethical regulations and identify the committee(s) approving the experiments.	Supp data P7
e)	For qPCR data provide information according to the Minimum Information for Publication of Quantitative Real-Time PCR Experiments (MIQE) guidelines	Supp data P6-7
3)	**Human subjects**	
a)	Identify the committee(s) approving the study protocol.	
b)	Include a statement confirming that informed consent was obtained from all subjects.	

c) For randomized studies report the clinical trial registration number (at ClinicalTrials.gov or equivalent).

d) For phase II and III randomized controlled trials:

I. Please refer to the CONSORT statement and submit the CONSORT checklist with your submission.

II. Include all version of the study protocol and statistical plan (to be published as supplementary information)

e) Identify the inclusion/exclusion criteria in the selection process for the patients included in the study

4) Statistics

a) State what statistical tests were completed and why — Supp data P8

b) Explain the sample size and how this size provides an adequate power to detect a pre-specified effect size.

5) Data deposition (Provide accession codes for deposited data)

a) When using public databases:

I. Identify the source and include a valid link — Supp data P4 and P6

II. When using databases that require permission, include a statement confirming that permission was obtained

b) Data deposition in a public repository is mandatory for:

I. Protein, DNA and RNA sequences — Supp data P4 and P12

II. Microarray data

Deposition is strongly recommended for many other datasets for which structured public repositories exist

JOURNAL
OF HEPATOLOGY

Journal of Hepatology
CTAT methods

Tables for a "Complete, Transparent, Accurate and Timely account" (CTAT) are now mandatory for all revised submissions. The aim is to enhance the reproducibility of methods.

- Only include the parts relevant to your study
- Refer to the CTAT in the main text as 'Supplementary CTAT Table'
- Do not add subheadings
- Add as many rows as needed to include all information
- Only include one item per row

If the CTAT form is not relevant to your study, please outline the reasons why:

1.1 Antibodies

Name	Citation	Supplier	Cat no.	Clone no.
RSK2		Cell signaling	5528	
Glutamine synthetase		BD Biosciences	610517	
phospho-ERK (Thr202/Tyr204)		Cell signaling	4376	
KI67		Cell signaling	12202	
ß-catenin		BD Biosciences	610153	
CK7		Abcam	181598	
RSK2		Santa Cruz Biotechnology	sc-1430	
ERK 1/2		Cell Signaling	9102	
phospho-ERK1/2 (Thr202/Tyr204)		Cell Signaling	9101	
β-actin		Sigma	A5060	

1.2 Cell lines

Name	Citation	Supplier	Cat no.	Passage no.	Authentication test method
Hep3B	Aden et al. Nature (1979) [PMID: 233137]	ATCC - USA			WES
Huh7	Nakabayashi et al Cancer Res (1982) [PMID: 6286115]	ATCC - USA			WES
PLC/PRF5	Alexander et al. S Afr Med J (1976) [PMID: 63998]	ATCC - USA			WES
SNU475	Park et al. Int J Cancer (1995) [PMID: 7543080]	ATCC - USA			WES

HepaRG	Gripon et al. PNAS (2002) [PMID: 12432097]	Gift from Philippe Merle and Fabien Zoulim (Inserm U1052, France)			WES
HepG2	Aden et al. Nature (1979) [PMID: 233137]	ATCC - USA			WES
Huh6	Doi et al. Gan (1976) [PMID: 57894]	RIKEN BioResource Center - Japan			WES

1.3 Organisms

Name	Citation	Supplier	Strain	Sex	Age	Overall n number
Rsk2$^{-/y}$ mice	Yang et al. Cell (2004) [PMID: 15109498]	André Hanauer	C57BL/6J	Male		
Axin1$^{fl/fl}$/AhCre mice	Feng et al. Gastroenterology (2012) [PMID: 22960659]	Trevor Dale	C57BL/6J	Male		

1.4 Sequence based reagents

Name	Sequence	Supplier
RPS6KA3 TaqMan predesigned assay	Hs00177936_m1	Life Technologies
Ribosomal 18S TaqMan predesigned assay	Hs03928990_g1	Life Technologies
Axin1 TaqMan predesigned assay	Mm01299058_m1	Life Technologies
Rps6ka3 TaqMan predesigned assay	Mm00455829_m1	Life Technologies
RPS6KA3 Forward primer (1)	AGGAGATTAACCCACAAACTGAAGA	Invitrogen
RPS6KA3 Reverse primer (1)	TCCAAAATAAGATACAACTTCCCTTCAG	Invitrogen
RPS6KA3 Forward primer (2)	ACAGTTTATTCCAGTCTATCGTTGAGA	Invitrogen
RPS6KA3 Reverse primer (2)	ACAGTTTATTCCAGTCTATCGTTGAGA	Invitrogen
RPS6KA3 Forward primer (3)	GTGCAGGACCAGATGGAGTT	Invitrogen
RPS6KA3 Reverse primer (3)	TGGATGCTGTCCATAACGAA	Invitrogen

RPS6KA3 Forward primer (4)	TCAATTGTTCAGCAGTTACACAGGA	Invitrogen
RPS6KA3 Reverse primer (4)	AGCAGCATCATAGCCTTGTCT	Invitrogen
RPS6KA3 Forward primer (5)	TGAGAGCGGAAAATGGTCTT	Invitrogen
RPS6KA3 Reverse primer (5)	CAGGGCTGTTGAGGTGATTT	Invitrogen
Rps6ka3 Forward primer	TTGTTGGTTTACTTTCTTTCGGTCTG	Invitrogen
Rps6ka3 Reverse primer	AAGATGATTGCTTTGCTTAGTTTA	Invitrogen
Axin1 Forward primer	CCTCAAGTAGACGGTACAACGAAGGCAGAG	Invitrogen
Axin1 Reverse primer	CTGTGCAGGAGCTCTACTAAGCCTCTACAC	Invitrogen
Cre Forward primer	TGACCGTACACCAAAATTTG	Invitrogen
Cre Reverse primer	ATTGCCCCTGTTTCACTATC	Invitrogen

1.5 Biological samples

Description	Source	Identifier
LICA-FR HCC dataset	PMID: 25822088 ; PMID: 29101368 ; PMID: 30531861 ; PMID: 31862487 ; PMID: 31206197	
TCGA HCC dataset	PMID: 28622513	
KOREAN HCC dataset	PMID: 24798001	
LIRI-JP HCC dataset	PMID: 27064257	

1.6 Deposited data

Name of repository	Identifier	Link
European Nucleotide Archive (ENA)	PRJEB59874	https://www.ebi.ac.uk/ena/browser/view/PRJEB59874

1.7 Software

Software name	Manufacturer	Version
GraphPad Prism	GraphPad Software	9
R software	R Foundation for Statistical Computing https://www.R-project.org	3.5.1
ImageLab software	Bio-Rad	5.2.1
Sequencher software	Gene codes corporation	
SDS software	Applied Biosystems	
Fluidigm Real-Time PCR Analysis software	Fluidigm	4.1.3

1.8 Other (e.g. drugs, proteins, vectors etc.)

Sorafenib	#S1040	Selleck Chemicals
Refametinib	#S1089	Selleck Chemicals
Trametinib	#S2673	Selleck Chemicals
PF-04691502	#S2743	Selleck Chemicals
Selumetinib	#S1008	Selleck Chemicals
Mirdametinib	#S1036	Selleck Chemicals
RPS6KA3 open reading frame	#OHS5900-224626707	Dharmacon
Empty vector	#OHS5833	Dharmacon
RPS6KA3 siRNA (1)	#s12279	Life Technologies
RPS6KA3 siRNA (2)	#s12280	Life Technologies
RPS6KA3 siRNA (3)	#s12280	Life Technologies
Block-iT Alexa Fluor Red siRNA	#14750100	Life Technologies

1.9 Please provide the details of the corresponding methods author for the manuscript:

sandra.rebouissou@inserm.fr

2.0 Please confirm for randomised controlled trials all versions of the clinical protocol are included in the submission. These will be published online as supplementary information.

NA

RSK2 inactivation cooperates with AXIN1 inactivation or ß-catenin activation to promote hepatocarcinogenesis

Samantha Schaeffer[1,2]*, Barkha Gupta[1,2]*, Anna-Line Calatayud[1,2]*, Julien Calderaro[3], Stefano Caruso[1,2], Théo Z. Hirsch[1,2], Laura Pelletier[1,2], Jessica Zucman-Rossi[1,2,4], Sandra Rebouissou[1,2].

* These authors contributed equally to this work.

Affiliations

1. Centre de Recherche des Cordeliers, Sorbonne Université, Inserm, Université Paris Cité, F-75006 Paris, France
2. Functional Genomics of Solid Tumors laboratory, équipe labellisée Ligue Nationale contre le Cancer
3. Service d'Anatomopathologie, Hôpital Henri Mondor, APHP, Institut Mondor de Recherche Biomédicale, F-94010 Créteil, France
4. Hôpital Européen Georges Pompidou, APHP, F-75015 Paris, France

Corresponding authors

Sandra Rebouissou, PhD. Centre de Recherche des Cordeliers. Functional Genomics of Solid Tumors. 15, Rue de l'Ecole de Médecine, 75006 Paris, France.
Phone : +33 6 73 11 74 93. Email : sandra.rebouissou@inserm.fr
Jessica Zucman-Rossi MD, PhD. Phone: +33 6 01 07 78 75. Email: jessica.zucman-rossi@inserm.fr

Conflict of interest

Nothing to disclose

Financial support

This work was supported by the ARC French foundation for Cancer Research**.** The team is supported by the Ligue Nationale Contre le Cancer (Equipe Labellisée). ALC was funded by a fellowship from the Ministry of Education and Research and from the ARC French foundation for Cancer Research, BG was funded by Institut National du Cancer (INCa), SC was funded by CARPEM and the Labex OncoImmunology, TZH was supported by a fellowship from Cancérôpole Ile-de-France and Fondation d'Entreprise Bristol-Myers Squibb pour la Recherche en Immuno-Oncologie and CARPEM.

Author contributions

Study concept and design: SR, JZR. Acquisition of data: ALC, SS, BG, LP. Analysis and data interpretation: ALC, SS, BG, SC, TZH, JC, LP, SR. Manuscript writing: SR, SS, BG, ALC and all. Obtained fundings: SR, JZR.

Data Availability Statement

RNA sequencing data reported in this study have been deposited in the ENA (European Nucleotide Archive) database (accession number: PRJEB59874).

Abstract

Background & Aims: Recurrent somatic mutations of *RPS6KA3* gene encoding for the serine/threonine kinase RSK2 were identified in hepatocellular carcinomas (HCC) suggesting its tumor suppressive function. Our goal was to demonstrate the tumor suppressor role of RSK2 in the liver and investigate the functional consequences of its inactivation.

Methods: We analyzed a series of 1151 human HCCs for RSK2 mutations and 20 other driver genetic alterations. We then modeled RSK2 inactivation in mice in various mutational contexts recapitulating or not those naturally found in human HCC, using transgenic mice and liver-specific carcinogens. These models were monitored for liver tumor appearance and subjected to phenotypic and transcriptomic analyzes. Functional consequences of RSK2 rescue were also investigated in a human RSK2 deficient HCC cell line.

Results: RSK2 inactivating mutations are specific of human HCC and frequently co-occur with AXIN1 inactivating or ß-catenin activating mutations. Modeling of these co-occurrences in mice showed cooperative effect in promoting liver tumors with transcriptomic profiles recapitulating those of human HCCs. By contrast, there was no cooperation in liver tumor induction between RSK2 loss and BRAF activating mutations chemically induced by diethylnitrosamine. In human liver cancer cells, we also showed that RSK2 inactivation confers some dependency to the activation of the RAS/MAPK signaling that can be targeted by MEK inhibitors.

Conclusions: Our study newly demonstrated the tumor suppressor role of RSK2 and its specific synergistic effect in hepatocarcinogenesis when its loss of function is specifically combined with AXIN1 inactivation or ß-catenin activation. Furthermore, we identified the RAS/MAPK pathway as a potential therapeutic target for RSK2-inactivated liver tumors.

Impact and implications

This study demonstrated the tumor suppressor role of RSK2 in the liver and showed that its inactivation specifically synergizes with AXIN1 inactivation or ß-catenin activation to promote the development of HCC with similar transcriptomic profiles as found in humans. Furthermore, this study highlights that activation of the RAS/MAPK pathway is one of the key signaling pathways mediating the oncogenic effect of RSK2 inactivation that can be targeted with already available anti-MEK therapies.

Keywords: hepatocellular carcinoma, RSK2, AXIN1, ß-catenin, mouse models, RAS/MAPK signaling

Electronic word count (with references): 7688

Number of Figures and Tables: 5 Figures

INTRODUCTION

Hepatocellular carcinoma (HCC) is the most common type of liver cancer in adults and rank fourth in cancer mortality worldwide [1]. Despite recent therapeutic progress, the prognosis of HCC patients remains poor, partly due to a lack of understanding of the oncogenic processes. Over the past decade, large-scale genomic studies in a wide variety of tumors have substantially improved the discovery of new cancer driver genes in HCCs and identified *RPS6KA3* as the most frequently mutated gene in the RAS/MAPK pathway [2,3]. More recently, recurrent *RPS6KA3* genetic alterations were also found in pediatric liver cancers [4–6].

RPS6KA3 is located on the X chromosome and codes for the serine/threonine kinase RSK2. Germline mutations resulting in loss of function of RSK2 have been previously associated with Coffin-Lowry syndrome (CLS), a rare genetic X-linked disorder characterized by cognitive impairment and skeletal abnormalities [7]. Somatic mutations identified in liver tumors also inactivate RSK2 activity suggesting its tumor suppressor function. RSK2 is activated downstream of the RAS/MAPK pathway by ERK1/2 and is able to phosphorylate many cytosolic and nuclear substrates, thus regulating many cellular functions, including proliferation, differentiation, cell death and survival [8]. However, the role of RSK2 inactivation in liver oncogenesis is still unclear and so far, most of the studies have rather suggested its oncogenic role in human tumors [9–11]. RSK2 is not only a downstream effector of the RAS/MAPK signaling but it also acts as a negative regulator of the pathway through inhibition of the SOS protein [12,13]. Several studies have reported a hyper-activation of the RAS/MAPK pathway following RSK2 inactivation [14–17] and a recent report has suggested that this activation could contribute to its oncogenic activity by supporting cholesterol biosynthesis in HCC [13]. However, the tumor suppressor function of RSK2 has not yet been demonstrated *in vivo* and further investigations are needed to better understand how its loss promotes hepatocarcinogenesis.

Here, we combined genomic analyzes of large sets of human HCCs with various experimental models where RSK2 was either inactivated in mice in different genetic contexts, recapitulating or not the natural mutational contexts found in human HCCs, or restored in a human RSK2 deficient HCC cell line.

Thus, we newly demonstrated the tumor suppressor role of RSK2 and its specific cooperative effect in liver carcinogenesis when combined with AXIN1 inactivation or ß-catenin activation, two other well-known HCC driver alterations. We also identified some dependency of RSK2 deficient HCC cells to the RAS/MAPK signaling pathway which can be therapeutically targeted by MEK1/2 inhibitors.

MATERIALS AND METHODS

Molecular and clinical analyses of human tumor samples

The global human HCC series includes 1151 samples from four different publicly available and previously described NGS datasets. Tumors other than HCC include 9542 samples from 34 different cancer types and are all part of the TCGA project available on cBioPortal.

Gene alteration and clinical data were extracted from cBioPortal or from original publications. Co-occurrence or mutual exclusivity between pairs of mutated genes in HCC was analyzed using the OncoPrinter cBioPortal tool.

RPS6KA3/RSK2 mRNA and protein expression were assessed in HCC by qRT-PCR and reverse-phase protein array (RPPA), respectively. Sanger sequencing of *RPS6KA3* was performed on cDNA for female samples to show that mutations occur on the transcribed/active X chromosome.

Survival analysis was performed in patients treated with liver resection using the Kaplan-Meier method.

Mouse models and immuno-histo-pathological analyses

Mice were housed in a specific pathogen-free facility and experiments were performed in accordance with French government regulations. All mice were males on an almost pure C57BL/6J background. Mice with constitutive and ubiquitous RSK2 inactivation (referred as *Rsk2*$^{-/y}$ genotype) were generated by Dr. André Hanauer [18] and AhCre floxed *Axin1* mice (referred as *Axin1*$^{fl/fl}$/AhCre genotype) were generated by Pr. Trevor Dale [19]. A third murine line was obtained by crossing the two transgenic models listed above to test for the cooperation between RSK2 and AXIN1 loss in liver tumor development.

AXIN1 was disrupted using a transcriptionally inducible Cre recombinase under the control of the *Cyp1a1* promoter (referred as AhCre) preferentially expressed in the liver, following intraperitoneal injections of ß-naphthoflavone.

For chemically induced mouse models of liver cancer, *Rsk2*$^{-/y}$ or wild-type mice were administered with single intraperitoneal injection of DEN (90 mg/kg), according to three different protocols: 1) at 6 weeks of age, followed by continuous oral administration of 0.05% phenobarbital (PB) in the drinking water or 2) at 2 weeks of age 3) at 6 weeks of age.

Genotypes and genes knockout were verified as described in the supplementary material and methods.

Mice livers were examined for tumor burden macroscopically and microscopically by HES and immunohistochemistry following standard procedures described in the supplementary material and methods.

Mouse liver transcriptomic analysis and mouse-human HCC expression profile comparison

A total of 12 non-tumor liver and 14 HCC mouse samples were analyzed by RNA-Sequencing. Libraries and sequencing were performed by Integragen SA and data have been deposited on the European Nucleotide Archive at EMBL-EBI: https://www.ebi.ac.uk/ena/browser/view/PRJEB59874

Mouse HCC transcriptomic profiles were compared with those of 196 human HCC based on correlation matrix performed on a 372-gene expression signature. Differentially expressed genes were identified using DESeq2 and GSEA analysis was performed using an in-house pipeline.

Functional analyses of RSK2 alteration in human HCC cell lines

RSK2 was stably overexpressed by lentiviral transduction or transiently knockdown by siRNA transfection in one and 6 human liver cancer cell lines, respectively. *RPS6KA3*/RSK2 mRNA and protein expression were checked by qRT-PCR and western-blot. Functional consequences of RSK2 alteration on cell survival, drug response and MAPK signaling were assessed by measuring mitochondrial activity and by western-blot.

Statistical analysis

Statistical analysis and data visualization were performed using both R software version 3.5.1 (R Foundation for Statistical Computing, Vienna, Austria. https://www.R-project.org) with Bioconductor packages and GraphPad Prism 9 software (GraphPad Software, Inc., La Jolla, CA). Comparison of a continuous variable in 2 groups was performed using either parametric test (t-test) if the variable was normally distributed or non-parametric test (Mann-Whitney). Qualitative data were compared using the Fisher's exact test and Chi-squared test to compare binary and non-binary categorical variables, respectively. Correlation analysis between continuous variables was performed using Pearson r correlation when both variables were normally distributed with the assumptions of linearity and homoscedasticity. All tests were two-tailed and *P*-value < 0.05 was considered as significant.

A more detailed description of the different procedures and analysis methodologies is provided in the supplementary material and methods and supplementary CTAT Table.

RESULTS

RPS6KA3/RSK2 meets the criteria of a tumor suppressor gene specifically in human HCC

We analyzed somatic mutations, amplifications and homozygous deletions of *RPS6KA3* gene in 35 different types of malignancies including 1151 human HCCs from four independent datasets with available NGS data **(Fig. 1A left panel)**. This analysis identified genomic alterations in *RPS6KA3* in 26 tumor types ranging from 0.3% to 7.8%. HCC was the fourth most frequently altered cancer with an overall frequency of 5.6%. The proportion of each class of alteration was variable across the different cancer types but in the most frequently altered (>5%), the predominance of homozygous deletions and truncating mutations was highly suggestive of an inactivating mutational spectrum. In HCCs, point mutations were distributed across all the RSK2 protein domains and were mostly truncating (60%), moreover, the majority of missenses mutations (87%) were predicted to be deleterious **(Fig. 1A right panel)**. This typical inactivating mutational spectrum was similar to the one found in patients with Coffin-Lowry syndrome carrying germline mutation of *RPS6KA3* [7,20] **(Fig. 1A right panel)**. By contrast, the distribution of RSK2 mutation classes was significantly different in non-HCC tumors with a low rate of truncating mutations (18%) and the presence of a high proportion of tolerated missense mutations, suggesting the absence of functional selective pressure against inactivating events **(Fig. 1A right panel)**. Moreover, it is striking that in tumors other than HCC, *RPS6KA3* mutations occurred frequently in the context of genetic instability in highly mutated tumors with a median mutation load 11-fold higher than in RSK2 non-mutated tumors (884 *vs* 79 mutations/tumor) **(Fig. 1A right panel),** contrasting with HCCs (89 *vs* 72 mutations/tumor). Of note, even in endometrial carcinoma, which is the most frequently altered cancer type for RSK2, 75% of the RSK2-mutated tumors exhibited *POLE* mutations, producing a high mutational burden, whereas only 4% of non-RSK2-mutated tumors were genetically altered for

POLE. Taken together, these results suggest that RSK2 mutations in non-HCC tumors could be potential passenger events, therefore, their functional consequence should be interpreted with caution in these cancers.

In line with the inactivating nature of the mutations found in HCCs, we identified a significant decrease in *RPS6KA3*/RSK2 mRNA and protein levels in HCCs genetically altered for *RPS6KA3* compared with non-altered HCCs **(Fig. 1B)**. Moreover, in HCCs developed in women, *RPS6KA3* somatic mutations were constantly found on the active X chromosome **(Fig. 1C)**. Consequently, in both men and women *RPS6KA3* mutations are predicted to lead to the complete inactivation of RSK2 and *RPS6KA3* thus meets the classic definition of a tumor suppressor gene. Overall, these results strongly support the tumor suppressor function of RSK2 specifically in the liver.

RPS6KA3 mutations frequently co-occur with _AXIN1_ or _CTNNB1_ mutations in HCC

Across all 1151 HCCs, by analyzing the co-occurrence of RSK2 inactivation with genetic alterations in 20 other well-established HCC driver genes we identified a significant enrichment of *AXIN1* inactivating alterations in RSK2 inactivated HCCs (30.6% *vs* 6.2%) **(Fig. 1D)**. Remarkably, activating mutations in *CTNNB1* that were mutually exclusive with *AXIN1* alterations were also frequently found with RSK2 inactivation (33.9%), whereas there was no significant enrichment. Thus, an alteration of the Wnt/ß-catenin pathway either through *AXIN1* inactivation or ß-catenin activation, was identified in 64.5% of the RSK2 inactivated HCCs *versus* 36.7% in RSK2 non-mutated HCCs (q-value<0.001), suggesting an oncogenic cooperation of these alterations in liver carcinogenesis. Surprisingly, genetic alterations in *APC* (also involved in the Wnt/ß-catenin pathway) were found to coexist with *AXIN1* or *CTNNB1* mutations in RSK2 inactivated HCCs **(Fig. 1D, right panel)**. At the transcriptomic level, the G1 subgroup that we have previously described to be characterized by an overexpression of liver progenitor markers [21] was significantly enriched in RSK2 inactivated HCCs, whereas the G4 subgroup belonging to the non-proliferation class was underrepresented **(Fig. 1E)**. Accordingly, patients with RSK2 inactivated HCCs had higher levels of serum alpha-fetoprotein **(Table S1)**. Remarkably, the G1 progenitor transcriptomic phenotype was driven by the co-occurrence of AXIN1 and RSK2 inactivation, whereas no obvious impact of RSK2 inactivation leading to change in transcriptomic subtype was observed in ß-catenin mutated HCCs, suggesting that the functional impact of RSK2 loss depends on the genetic context **(Fig. 1E and Fig. S1)**. No significant relation with other clinical features were identified in RSK2 altered HCCs **(Fig. S2 and Table S1)**.

RSK2 inactivation cooperates with AXIN1 inactivation or ß-catenin activation to induce liver tumors in mice

In C57BL/6J mice, the ubiquitous and constitutive inactivation of RSK2 alone is not sufficient to induce liver tumors [18]. Thus, in order to investigate the tumor suppressor role of RSK2 in the liver, we generated three different mouse models combining RSK2 inactivation with an additional genetic alteration using transgenic mice and liver-specific chemical carcinogens. In the first two models, RSK2 inactivation was combined either with *Axin1* bi-allelic inactivation induced in the liver at 6 weeks of age using the Cre/loxP system, or with ß-catenin activation induced by diethylnitrosamine (DEN) administrated at 6 weeks of age, followed by continuous phenobarbital (PB) treatment, yielding 80% of *Ctnnb1*-mutated tumors [22], thus recapitulating the two major oncogenic events co-occurring with RSK2 inactivation that we have identified in human HCCs **(Fig. 2A)**. We also generated a third model by treating juvenile mice with DEN alone, which is known to induce liver tumors with BRAF activating mutations in approximately

90% of cases in the C57BL/6J background [23], to test a more artificial context not found in human HCCs and to assess the specificity of oncogenic cooperations with RSK2 inactivation **(Fig. 2A)**.

At 12 months of age, we identified a significantly higher penetrance of liver tumors reaching 62.5% in mice with double inactivation of RSK2 and AXIN1 (*Rsk2*$^{-/y}$; *Axin1*$^{fl/fl}$/AhCre) compared with mice harboring AXIN1 (*Rsk2*^{wt}; *Axin1*$^{fl/fl}$/AhCre=8.3%) or RSK2 (*Rsk2*$^{-/y}$; *Axin1*^{wt}/AhCre=0%) inactivation alone and wild-type mice (*Rsk2*^{wt} ; *Axin1*^{wt}/AhCre=0%) **(Fig. 2A)**. There was no significant difference in liver tumor burden between the four genotypes at 9 months **(Fig. S3A)** and no liver tumor development was observed in the control mice with monogenic inactivation of *Axin1* alone (*Rsk2*^{wt}; *Axin1*$^{wt/fl}$/AhCre n=9) or combined with RSK2 inactivation (*Rsk2*$^{-/y}$; *Axin1*$^{wt/fl}$/AhCre n=11).

In the DEN/PB model, the incidence of liver tumors was also significantly higher in *Rsk2*$^{-/y}$ mice, compared with wild-type mice at 9 (**Fig. S3A**, 87.5% *vs* 20%) and 12 months (**Fig. 2A**, 100% *vs* 50%). By contrast, in juvenile mice treated with DEN alone, there was no difference in liver tumor development between *Rsk2*$^{-/y}$ (75%) and wild-type mice (80%) at 6 months **(Fig. 2A)**. Because tumor incidence was high in this model, we also injected 6-weeks-old adult mice with DEN in order to induce a lower tumor burden and still observed a similar frequency of liver tumors between *Rsk2*$^{-/y}$ (25%) and wild-type mice (27.3%) at 12 months **(Fig. S3B)**.

In the three mouse models analyzed, there was no significant difference in the number of liver nodules per mouse between genotypes **(Fig. 2A and Fig. S3A)** and the histology was consistent with HCC in most cases with a moderate to high KI67 proliferation index **(Fig. 2A)**. However, a significantly lower KI67 index was observed in liver tumors developed in *Rsk2*$^{-/y}$ mice treated with DEN and PB compared with wild-type mice **(Fig. 2A)**.

We also analyzed three immunohistochemical markers to characterize the liver tumors developed in the different genotypes of each mouse model.

In the DEN/PB model, as expected, a large majority of the tumors in both *Rsk2*$^{-/y}$ and wild-type mice showed a glutamine synthetase (GS) positive staining and nuclear accumulation of ß-catenin that was more frequently observed in *Rsk2*$^{-/y}$ genotype, thereby reflecting a potent activation of the β-catenin pathway **(Fig. 2)**. We also confirmed the presence of classical ß-catenin activating mutations in this model by RNA-sequencing in three tumors from the two *Rsk2* genotypes **(Fig. S4A)**. By contrast, most tumors developed in the DEN model and all tumors developed in the context of AXIN1 inactivation were negative for GS and ß-catenin staining independent of *Rsk2* genotype **(Fig. 2)**. Similar finding has been reported in the previous studies in the literature [19,24]. Furthermore, we found no transcriptional deregulation in 10 canonical target genes (n=10) and 9 other liver-specific target genes of ß-catenin in tumors with AXIN1 inactivation, regardless of *Rsk2* genotype **(Fig. S5A)**.

In the DEN model, liver tumors were characterized by more frequent positive staining for phospho-ERK with an increased H-score compared with the two other mouse models (transgenic and DEN/PB) **(Fig. 2)**. These results are consistent with the well-known induction of BRAF activating mutations in this model that we confirmed by RNA-sequencing and Sanger sequencing in 4/5 (80%) of the tumors of each *Rsk2* genotype **(Fig. S4A)**. Furthermore, in the DEN model, higher positivity of phospho-ERK (H-score) was observed in liver tumors from *Rsk2*$^{-/y}$ mice compared with wild-type mice suggesting that loss of function of RSK2 potentiates activation of the RAS/MAPK pathway in BRAF activated tumors, as we previously showed in the HepG2 cell line with an activating mutation in NRAS [14,25] **(Fig. 2)**. In the DEN/PB model phospho-ERK positivity was noted only in a small fraction of tumors, with no significant difference between *Rsk2* genotypes, even when the comparison was restricted to only GS and/or nuclear ß-catenin positive tumors to limit the heterogeneity of the model **(Fig. 2 and**

Fig. S3A and S3C). Strikingly, in mice with double inactivation of RSK2 and AXIN1 (*Rsk2*$^{-/y}$; *Axin1*$^{fl/fl}$/AhCre), phospho-ERK positivity was predominantly found in the larger nodules. Interestingly, we identified a typical activating mutation of HRAS by RNA-sequencing in three independent tumors from two mice **(Fig. S4B)**. Notably, the two nodules occurring in the same mouse were mutated at the same position but with a different amino-acid substitution, suggesting independent mutational events **(Fig. S4B)**. Altogether, these results indicate that HRAS activating mutations are specifically selected during liver tumor progression after double inactivation of RSK2 and AXIN1, as no *Hras* mutation was identified in the larger nodules analyzed in the other two mouse models (DEN/PB and DEN alone).

As previously described [19], in the non-tumor livers of AXIN1 inactivated mice, irrespective of *Rsk2* genotype, we found a significant increase in cellular atypia and hepatomegaly with a higher liver/body weight ratio when compared with RSK2 inactivated (*Axin1*^{wt}/AhCre ; *Rsk2*$^{-/y}$) and wild-type (*Axin1*^{wt}/AhCre ; *Rsk2*^{wt}) mice **(Fig. 2A and Fig. S3A)**.

Overall, our results demonstrate that RSK2 inactivation synergizes with AXIN1 inactivation to promote liver carcinogenesis and also support its cooperative effect with ß-catenin activation but not with BRAF activation ; thus validating the co-occurrences found in human HCCs. Moreover, RSK2 inactivation alone is not a strong inducer of the RAS/MAPK signaling in tumors, but its co-occurrence with another triggering event may potentiate this activation.

Mouse HCCs from the different oncogenic cooperation models with RSK2 loss transcriptomically match human HCCs

For each of the three mouse models, we selected the most advanced liver tumors for transcriptomic analysis. We analyzed a total of 14 HCC samples from 10 mice including at least two independent nodules for each genotype, with an exception of one condition for which two parts of the same tumor were analyzed because only one sample was available **(Table S2)**. Principal component analysis (PCA) and unsupervised hierarchical clustering on the 1000 most variable genes divided the mouse HCC samples into two major groups **(Fig. 3A)**. The first included mouse HCCs with ß-catenin activation or AXIN1 inactivation and was grouped according to their genotype. The second group was defined by HCCs developed in mice inactivated for both RSK2 & AXIN1 and HCCs from the DEN model including *Rsk2*$^{-/y}$ & wild-type genotypes. This group was also characterized by activating mutations in the RAS/MAPK signaling **(Fig. 3A)**.

We then searched for similarities between the transcriptomic profiles of mouse and human HCCs using a 372-gene expression signature that classifies human HCCs into 6 molecular groups from G1 to G6 as previously described [21] **(Table S3)**. Based on this transcriptomic signature, we generated a pairwise correlation matrix between a set of 196 human HCCs (LICA-FR cohort) and the 14 mouse HCC samples. Hierarchical clustering of pairwise correlation coefficients allowed us to group the mouse and human HCCs into two major clusters based on their similarity **(Fig. 3B)**. The two mouse clusters were almost similar to those previously identified in the unsupervised analysis except for one sample (1284_T1) that was shifted from the transcriptomic group **(Fig. 3B)**. The first group of mice HCCs with ß-catenin activation (DEN/PB model) or AXIN1 inactivation corresponded to the “non-proliferation” class of human HCCs **(Fig. 3B)**. By contrast, the second cluster of mouse HCCs developed in the RSK2/AXIN1 double knockout and DEN models was associated with the more aggressive “proliferation” class of human HCCs, mainly characterized by *TP53* inactivating mutations and G1 to G3 transcriptomic groups **(Fig. 3B)**. To test the strength of the association between the mouse models and each of the 6 human HCC transcriptomic groups, we searched for statistical enrichment in the proportion of human HCCs with the 372-

gene expression signature that was significantly correlated with each mouse HCC sample **(Fig. 3C)**.

This analysis revealed that mouse HCCs developed in the DEN/PB model were strongly associated with ß-catenin mutated human HCCs from G5-G6 groups, irrespective of their *Rsk2* genotype, as seen in humans **(Fig. 3C and Fig S1A)**. By contrast, tumors with AXIN1 inactivation alone showed no association with any of the 6 human transcriptomic groups **(Fig. 3C)**. Interestingly, as seen in human HCCs, tumors in the double knock-out model in mice also showed similarity to the G1 human transcriptomic group; with the exception of one sample demonstrating similar profile as ß-catenin activated human HCCs. This could be related to the tumor heterogeneity with a large tumor area showing FNH-like pattern characterized by typical GS staining in map-like pattern, without nuclear ß-catenin accumulation and without *Ctnnb1* mutation **(Fig. 3C and Fig. S6)** [26].

Tumors developed in the DEN model were mostly heterogeneous, regardless of their *Rsk2* genotype, but were often associated with G1 and/or G3 human HCC transcriptomic groups **(Fig. 3C)**. Overall, our results show that mouse HCCs developed in the context of RSK2 inactivation combined with either AXIN1 inactivation or ß-catenin activation, which recapitulates the natural genetic co-occurrence found in human HCCs, also transcriptionally mimic these HCCs subgroups.

Pretumor impact of RSK2 and/or acute AXIN1 inactivation in adult mouse liver

We studied the short-term consequences of RSK2 and/or AXIN1 inactivation prior to tumor development in the liver of 6 weeks old mice.

As previously described [19], we found a significant 5-fold increase in KI67 proliferation index following acute loss of AXIN1 alone (after 4 days of BNF treatment) (mean=18.4%) compared to wild-type mice (mean=3.9%), whereas no difference was observed for RSK2 inactivated mice (mean=4.1%) **(Fig. 4A)**. Interestingly, this increase was even more pronounced (2-fold) when both AXIN1 and RSK2 were inactivated (mean=35.8%) indicating that concomitant loss of these two genes has a synergistic effect in promoting liver cell proliferation.

In addition, immunohistochemical staining of CK7 revealed different morphological changes in the liver depending on the genotype with an increase in number of oval cells per portal tract in *Rsk2*$^{-/y}$ mice (mean=21.3 *vs* 14 in wild-type mice **Fig. S7**) and a significant enlargement of bile ducts in AXIN1 inactivated mice possibly related to hyper-proliferation of cholangiocytes (mean=32.6 µm *vs* 17.5 µm in wild-type mice) **(Fig. 4A)**. These two features were also commonly found in the *Rsk2*$^{-/y}$; *Axin1*$^{fl/fl}$/AhCre double knock-out mice **(Fig. 4A)**. PCA analysis of liver transcriptomic profiles on the 500 most variable genes revealed four distinct groups corresponding to each mouse genotype **(Fig. 4B)**. RSK2 inactivated livers were more similar to wild-type livers, whereas livers inactivated for AXIN1 alone or combined with RSK2 loss showed more divergent profiles **(Fig. 4B)**. Consistent with these results, differential expressed genes (DEGs) analysis identified only 132 differentially expressed genes between RSK2 inactivated and wild-type mouse livers with a large predominance of down-regulated genes (80%) **(Fig. 4C and Table S4)**, while AXIN1 inactivation alone or combined with RSK2 loss had a greater effect on the transcriptomic profile with 2723 and 1906 DEGs, respectively, compared to wild-type livers with an almost equal distribution between over and under-expressed genes **(Fig. 4C and Table S4)**. We also identified 1439 DEGs between normal livers deficient for AXIN1 alone and those deficient for both AXIN1 and RSK2 **(Fig. 4C and Table S4)**. We then performed a gene set enrichment analysis (GSEA) comparing the three genotypes compared to wild-type livers that identified inflammation/immune response and cell cycle/proliferation as the two main enriched categories of gene sets accounting for 20 to 25%

of the whole significant gene sets **(Table S5)**. Inflammation/Immune response gene sets were particularly enriched in RSK2 inactivated livers with a slight over-representation of positive normalized enrichment score (NES), while negative NES were enriched in mice livers inactivated for both RSK2 and AXIN1 indicating a decrease in inflammatory processes specifically driven by the concomitant loss of RSK2 and AXIN1 **(Fig. 4D).** This decrease was also significant in RSK2/AXIN1 deficient livers compared to those only inactivated for AXIN1 supporting the role of RSK2 loss in the inflammatory process deficiency specifically in the context of AXIN1 inactivation **(Fig. 4D)**. Surprisingly, cell cycle and proliferation related gene sets were all negatively enriched in RSK2 inactivated livers. This contrasts with AXIN1 and RSK2/AXIN1 inactivated livers, that both demonstrated strong positive enrichment with higher significance when both AXIN1 and RSK2 were inactivated, although there was no significant difference when comparing RSK2/AXIN1 deficient livers with AXIN1 **(Fig. 4D)**. These results are consistent with the proliferation index analysis. Finally, we identified no obvious transcriptional deregulation of ß-catenin target genes (except *Lect2*) in AXIN1 inactivated livers, regardless of *Rsk2* genotype (**Fig. S4B**).

RSK2 deficiency in human liver cancer cells results in some dependency to the RAS/MAPK signaling

Several studies have shown the inhibitory role of RSK2 on the RAS/MAPK pathway [12,13]. So, we wondered whether activation of the RAS/MAPK signaling mediated by the loss of RSK2 would render liver tumor cells dependent on this pathway for their growth. For this purpose, we restored the expression of RSK2 in the Hep3B cell line derived from a human HCC that is constitutively deficient for RSK2 through a gene deletion [25]. This cell line also harbors a homozygous deletion of *AXIN1* gene and was classified in the G1 HCC transcriptomic group, thus fully recapitulating one of the natural molecular context of RSK2 inactivation found in human HCCs [25] **(Fig. 5A)**. We showed that stable rescue of RSK2 expression in Hep3B cells by lentiviral transduction of the *RPS6KA3* open reading frame resulted in a significant decrease in ERK phosphorylation and cell viability **(Fig. 5B)**. Subsequently, we used pharmacological inhibitors to assess the dependency of tumor cells to the RAS/MAPK signaling related to the loss of RSK2 in the parental cells and after RSK2-rescue.

Parental Hep3B cells deficient for RSK2, whether or not transduced with the empty vector, demonstrated high basal sensitivity to the two MEK1/2 inhibitors trametinib and refametinib and showed moderate sensitivity to the RAF inhibitor sorafenib **(Fig. 5B)**. Interestingly, RSK2 rescue was able to decrease sensitivity to the three RAS/MAPK signaling inhibitors while sensitivity to the PF-04691502 inhibitor targeting the PI3K/mTOR pathway remained unchanged compared to the RSK2-deficient parental cells supporting the specific role of RSK2 in modulation of the RAS/MAPK activity **(Fig. 5B)**. All these results indicate that the loss of RSK2 function confers a certain dependence of liver cancer cells to the activation of the RAS/MAPK signaling and that MEK inhibitors could be interesting candidate therapies to target RSK2-inactivated HCCs. We also silenced RSK2 by siRNA in 6 human liver cancer cell lines. Although there was no increase in cell survival following RSK2 knockdown, ERK phosphorylation was enhanced and can be efficiently inhibited by MEK inhibitors (**Fig. S8**).

DISCUSSION

Although RSK2 has been described so far as an onco-kinase, the inactivating nature of RSK2 mutations identified in human HCCs similar to those found in CLS patients strongly supports its tumor suppressive function, in accordance with the '20/20' rule defining a gene as a tumor suppressor as long as >20% of its mutations are inactivating [27]. In other types of tumors, we showed that RSK2 mutational spectrum was significantly different and mutations occurred preferentially in hyper-mutated tumors which argues in favor of passenger events. Apart from adult HCCs, recurrent RSK2 inactivating mutations have also been reported in pediatric liver cancers, including HCCs and hepatoblastoma [4–6]. Hence, these findings suggest a liver-specific tumor suppressor function of RSK2.

The role of RSK2 in the negative control of the RAS/MAPK signaling is now well established [12–17]. RSK2 has been shown to phosphorylate the guanine nucleotide exchange factor SOS leading to its dissociation from Grb2 and thereby suppressing RAS activity and downstream ERK activation [12,13]. Accordingly, in the present study we showed that this negative feedback was restored after RSK2 rescue in a RSK2-deficient HCC cell line. Moreover, we also demonstrated that RSK2 loss rendered liver tumor cells partially dependent on the activation of the RAS/MAPK pathway for their growth, corroborating previous findings [13]. Apart from the activation of the RAF/MEK/ERK pathway, the second best-characterized RAS effector family is phosphoinositide 3-kinases (PI3Ks), which also play an important role in RAS-mediated cell survival and proliferation [28]. However, in our study, sensitivity to a dual PI3K/mTOR inhibitor was not reversed after RSK2 rescue in contrast to MEK and RAF inhibitors, suggesting that PI3K/mTOR activation was independent of RSK2 activity. Hence, all these results argue in favor of a major role of the abnormal activation of the RAS/MAPK pathway in the oncogenic effect mediated by RSK2 loss of function. However, we showed that RSK2 inactivation alone was not able to promote liver carcinogenesis in mice. Surprisingly, when RSK2 inactivation was combined with BRAF-activating mutations chemically induced by the liver-specific carcinogen DEN, there was no increase in the incidence of liver tumors. This lack of oncogenic cooperation between RSK2 loss and BRAF activating mutations may be related to their functional redundancy, as they both converge towards an activation of the RAS/MAPK signaling. This may also explain why this co-occurrence has never been found in human HCCs. Although we showed in mouse liver tumors that loss of RSK2 was able to potentiate RAS/MAPK activation induced by BRAF activating mutations, this was not sufficient to accelerate carcinogenesis, suggesting that other signaling pathways need to be concomitantly altered to provide a selective advantage. Consistent with this hypothesis, several reports have shown that oncogenic mutations in RAS alone, were not sufficient to promote HCC development in mice [29–32]. In humans, by analyzing a large set of HCCs, we identified frequent co-occurrence between RSK2 inactivation and AXIN1 inactivating mutations or ß-catenin activating mutations, two well-known and mutually exclusive HCC driver alterations, both of which are expected to lead to an abnormal activation of the Wnt/ß-catenin pathway. Thus, these results suggest a potential cooperation between the RAS/MAPK and Wnt/ß-catenin pathways in the liver tumor development. Consistent with this hypothesis, we found a cooperative effect in liver tumor induction when modeling these two co-occurrence pairs in mice, combining RSK2 inactivation with either genetically induced AXIN1 inactivation or ß-catenin activation obtained in a chemically induced carcinogenesis model enriched in ß-catenin activating mutations.

Interestingly, previous studies have already demonstrated that RAS and ß-catenin oncogenic mutants act synergistically to yield HCC in mice [31,32]. However, the role of AXIN1

inactivation in ß-catenin mediated hepatocarcinogenesis is still debated. In humans, HCCs carrying activating ß-catenin mutations and those with inactivating AXIN1 mutations have very different transcriptomic signatures [3]. In mice, we confirmed the absence of induction of the canonical and liver specific Wnt/ß-catenin targets such as GS, after conditional inactivation of AXIN1 as previously described [19,24], contrary to ß-catenin mutated tumors. However, a role of ß-catenin activation related to the AXIN1 loss cannot be completely excluded. Indeed, several studies using a reporter gene assay have demonstrated an increased transcriptional activity of ß-catenin in human HCC cell lines harboring AXIN1 inactivating mutations, albeit at a lower level than in cell lines with ß-catenin activating mutations [33,34]. In agreement with these findings, more recently Qiao *et al.* identified a weak activation of the Wnt/β-Catenin cascade in mice HCCs where AXIN1 was suppressed concomitantly with c-MET overexpression [35]. Moreover, they initially demonstrated in this model that HCC driven by the loss of AXIN1 requires an intact β-Catenin [35]. Another study also reported a role of NOTCH and YAP signaling pathways in liver carcinogenesis mediated by AXIN1 loss [24]. Whether these different pathways cooperate with RSK2 loss remains to be investigated.

Unexpectedly, in our mouse model inactivated for both RSK2 and AXIN1, we specifically identified HRAS activating mutation as a third mutational hit involved in HCC progression correlating with larger nodules highly positive for phospho-ERK. This may explain the long latency and incomplete penetrance in this model, as additional genetic events may be required for the development of liver tumors. In humans, we showed that the co-occurrence of RSK2 and AXIN1 mutations was strongly associated with the G1 transcriptomic group. Furthermore, in a previous work, we identified an enrichment of phospho-ERK positive tumors in the G1 transcriptomic subgroup, which may partially mimic what we observed in our mouse model [36]. Although no RAS mutation has been identified in this subgroup of HCC, other molecular alterations may contribute to the increased level of RAS/MAPK pathway activation, such as the overexpression of IGF2 generally found in the G1 subgroup and previously shown as an epigenetic oncodriver in human HCCs [37]. Based on these results, we can propose a model of tumor progression in which RSK2 loss that induces mild activation of RAS/MAPK pathway would be required at an early stage of carcinogenesis to allow liver cell survival and prevent oncogene-induced senescence but higher activation may be necessary for tumor progression through the acquisition of an additional RAS/MAPK activating event. Interestingly, findings in a recent study support this hypothesis showing that higher RAS/MAPK signaling intensity was associated with subclonal growth advantage in a mouse model of primary and metastatic HCC [38].

In addition, we also showed that transcriptomic profiles of mouse HCCs generated in the context of RSK2 inactivation either with AXIN1 loss or ß-catenin activation, recapitulated those of human HCCs with similar genetic contexts suggesting that our preclinical models are suitable for studying these HCC subclasses. Finally, at a pretumor stage, we showed that the concomitant loss of RSK2 and AXIN1 leads to greater proliferation of liver cells together with bile duct enlargement and an increase in number of oval cells known as hepatic progenitors. These short-term phenotypic changes may favor the subsequent promotion of liver tumors as well as the decrease in inflammatory processes identified specifically in this context.

In conclusion, we provided new evidence for the tumor suppressor role of RSK2 in the liver and demonstrated that its loss of function specifically synergized with AXIN1 inactivation or ß-catenin activation in HCC development. Our study also well illustrated the crucial role of genetic contexts in the promotion of carcinogenesis, emphasizing that only the right oncogenic cooperations can provide selective advantage. Furthermore, this work identifies the

RAS/MAPK pathway as a potential promising therapeutic target for RSK2 inactivated HCCs with already available therapies. However, whether targeting this pathway alone will be sufficient or whether it will need to be combined with another therapy remains to be further explored.

Abbreviations

Alt., genetic alteration; BNF, β-naphthoflavone; CLS, Coffin-Lowry syndrome; DEG, differentially expressed genes; DEN, diethylnitrosamine; ERK, extracellular signal-regulated kinase; GS, glutamine synthetase; GSEA, gene set enrichment analysis; HCC, hepatocellular carcinoma; HES, hemalun-eosin-safran; IHC, immunohistochemistry; M, mutated; MAPK, mitogen-activated protein kinase; MEK, mitogen-activated protein kinase kinase; MOI, multiplicity of infection; NES, normalized enrichment score; NM, non-mutated; NTL, non-tumor liver; PB, phenobarbital; PCA, principal component analysis; RSK2, p90 ribosomal S6 kinase; SOS, son of sevenless

Acknowledgments

We warmly thank André Hanauer (IGBMC, France) who provided us the RSK2 inactivated mice. We are also very grateful to Trevor Dale who provided us the AXIN1 transgenic mice and Victoria Marsh (Cardiff University, United Kingdom) for her advice with managing them. We also thank Véronique Parietti-Montcuquet, Martine Chopin for their technical support at animal facility, Emilie Gelabale and Laure Caruana for their assistance in mouse management, histology and immunohistochemistry. We are grateful to the CRC (Cordelier's Research Center) core facilities for the technical and methodological help, assistance and support. We also thank Sabine Rajkumar, Caroline Lecerf, Floriane Bard, and Audrey Criqui for acquisition of reverse phase protein array data. We thank all the clinicians, surgeons and pathologists who have participated in collecting human tumor samples from the LICA-FR cohort: Jean Saric, Christophe Laurent, Laurence Chiche, Brigitte Le Bail, Claire Castain (CHU Bordeaux), Alexis Laurent, Daniel Cherqui, Daniel Azoulay (CHU Henri Mondor, Créteil, APHP), Jean-Charles Nault, Marianne Ziol, Nathalie Ganne-Carrié, Olivier Seror and Pierre Nahon (Jean Verdier Hospital, Bondy, APHP). We also thank the Réseau national CRB Foie (BB-0033-0085), the tumor banks of CHU Bordeaux (BB-0033-00036), Jean Verdier Hospital (APHP) and CHU Henri Mondor (APHP) for contributing to the tissue collection.

References

Author names in bold designate shared co-first authorship

[1] Villanueva A. Hepatocellular Carcinoma. N Engl J Med 2019;380:1450–62. https://doi.org/10.1056/NEJMra1713263.

[2] **Guichard C, Amaddeo G, Imbeaud S**, Ladeiro Y, Pelletier L, Maad IB, et al. Integrated analysis of somatic mutations and focal copy-number changes identifies key genes and pathways in hepatocellular carcinoma. Nat Genet 2012;44:694–8. https://doi.org/10.1038/ng.2256.

[3] Rebouissou S, Nault J-C. Advances in molecular classification and precision oncology in hepatocellular carcinoma. J Hepatol 2020;72:215–29. https://doi.org/10.1016/j.jhep.2019.08.017.

[4] Haines K, Sarabia SF, Alvarez KR, Tomlinson G, Vasudevan SA, Heczey AA, et al. Characterization of pediatric hepatocellular carcinoma reveals genomic heterogeneity and diverse signaling pathway activation. Pediatr Blood Cancer 2019;66:e27745. https://doi.org/10.1002/pbc.27745.

[5] **Hirsch TZ, Pilet J, Morcrette G**, Roehrig A, Monteiro BJE, Molina L, et al. Integrated Genomic Analysis Identifies Driver Genes and Cisplatin-Resistant Progenitor Phenotype in Pediatric Liver Cancer. Cancer Discov 2021;11:2524–43. https://doi.org/10.1158/2159-8290.CD-20-1809.

[6] **Sumazin P, Peters TL, Sarabia SF**, Kim HR, Urbicain M, Hollingsworth EF, et al. Hepatoblastomas with carcinoma features represent a biological spectrum of aggressive neoplasms in children and young adults. J Hepatol 2022:S0168-8278(22)00275-6. https://doi.org/10.1016/j.jhep.2022.04.035.

[7] Delaunoy J, Abidi F, Zeniou M, Jacquot S, Merienne K, Pannetier S, et al. Mutations in the X-linked RSK2 gene (RPS6KA3) in patients with Coffin-Lowry syndrome. Hum Mutat 2001;17:103–16. https://doi.org/10.1002/1098-1004(200102)17:2<103::AID-HUMU2>3.0.CO;2-N.

[8] Romeo Y, Zhang X, Roux PP. Regulation and function of the RSK family of protein kinases. Biochem J 2012;441:553–69. https://doi.org/10.1042/BJ20110289.

[9] Kang S, Dong S, Gu T-L, Guo A, Cohen MS, Lonial S, et al. FGFR3 activates RSK2 to mediate hematopoietic transformation through tyrosine phosphorylation of RSK2 and activation of the MEK/ERK pathway. Cancer Cell 2007;12:201–14. https://doi.org/10.1016/j.ccr.2007.08.003.

[10] Kang S, Elf S, Lythgoe K, Hitosugi T, Taunton J, Zhou W, et al. p90 ribosomal S6 kinase 2 promotes invasion and metastasis of human head and neck squamous cell carcinoma cells. J Clin Invest 2010;120:1165–77. https://doi.org/10.1172/JCI40582.

[11] Xian W, Pappas L, Pandya D, Selfors LM, Derksen PW, de Bruin M, et al. Fibroblast growth factor receptor 1-transformed mammary epithelial cells are dependent on RSK activity for growth and survival. Cancer Res 2009;69:2244–51. https://doi.org/10.1158/0008-5472.CAN-08-3398.

[12] Douville E, Downward J. EGF induced SOS phosphorylation in PC12 cells involves P90 RSK-2. Oncogene 1997;15:373–83. https://doi.org/10.1038/sj.onc.1201214.

[13] Chan L-K, Ho DW-H, Kam CS, Chiu EY-T, Lo IL-O, Yau DT-W, et al. RSK2-inactivating mutations potentiate MAPK signaling and support cholesterol metabolism in hepatocellular carcinoma. J Hepatol 2021;74:360–71. https://doi.org/10.1016/j.jhep.2020.08.036.

[14] **Schulze K, Imbeaud S, Letouzé E**, Alexandrov LB, Calderaro J, Rebouissou S, et al. Exome sequencing of hepatocellular carcinomas identifies new mutational signatures and potential therapeutic targets. Nat Genet 2015;47:505–11. https://doi.org/10.1038/ng.3252.

[15] Schneider A, Mehmood T, Pannetier S, Hanauer A. Altered ERK/MAPK signaling in the hippocampus of the mrsk2_KO mouse model of Coffin-Lowry syndrome. J Neurochem 2011;119:447–59. https://doi.org/10.1111/j.1471-4159.2011.07423.x.

[16] Dufresne SD, Bjørbaek C, El-Haschimi K, Zhao Y, Aschenbach WG, Moller DE, et al. Altered extracellular signal-regulated kinase signaling and glycogen metabolism in skeletal muscle from p90 ribosomal S6 kinase 2 knockout mice. Mol Cell Biol 2001;21:81–7.

https://doi.org/10.1128/MCB.21.1.81-87.2001.
[17] Clark CJ, McDade DM, O'Shaughnessy CT, Morris BJ. Contrasting roles of neuronal Msk1 and Rsk2 in Bad phosphorylation and feedback regulation of Erk signalling. J Neurochem 2007;102:1024–34. https://doi.org/10.1111/j.1471-4159.2007.04601.x.
[18] Yang X, Matsuda K, Bialek P, Jacquot S, Masuoka HC, Schinke T, et al. ATF4 is a substrate of RSK2 and an essential regulator of osteoblast biology; implication for Coffin-Lowry Syndrome. Cell 2004;117:387–98. https://doi.org/10.1016/s0092-8674(04)00344-7.
[19] Feng GJ, Cotta W, Wei XQ, Poetz O, Evans R, Jardé T, et al. Conditional disruption of Axin1 leads to development of liver tumors in mice. Gastroenterology 2012;143:1650–9. https://doi.org/10.1053/j.gastro.2012.08.047.
[20] Delaunoy JP, Dubos A, Marques Pereira P, Hanauer A. Identification of novel mutations in the RSK2 gene (RPS6KA3) in patients with Coffin-Lowry syndrome. Clin Genet 2006;70:161–6. https://doi.org/10.1111/j.1399-0004.2006.00660.x.
[21] Boyault S, Rickman DS, de Reyniès A, Balabaud C, Rebouissou S, Jeannot E, et al. Transcriptome classification of HCC is related to gene alterations and to new therapeutic targets. Hepatology 2007;45:42–52. https://doi.org/10.1002/hep.21467.
[22] Aydinlik H, Nguyen TD, Moennikes O, Buchmann A, Schwarz M. Selective pressure during tumor promotion by phenobarbital leads to clonal outgrowth of beta-catenin-mutated mouse liver tumors. Oncogene 2001;20:7812–6. https://doi.org/10.1038/sj.onc.1204982.
[23] Buchmann A, Karcier Z, Schmid B, Strathmann J, Schwarz M. Differential selection for B-raf and Ha-ras mutated liver tumors in mice with high and low susceptibility to hepatocarcinogenesis. Mutat Res 2008;638:66–74. https://doi.org/10.1016/j.mrfmmm.2007.08.015.
[24] **Abitbol S, Dahmani R**, Coulouarn C, Ragazzon B, Mlecnik B, Senni N, et al. AXIN deficiency in human and mouse hepatocytes induces hepatocellular carcinoma in the absence of β-catenin activation. J Hepatol 2018;68:1203–13. https://doi.org/10.1016/j.jhep.2017.12.018.
[25] **Caruso S, Calatayud A-L, Pilet J**, La Bella T, Rekik S, Imbeaud S, et al. Analysis of Liver Cancer Cell Lines Identifies Agents With Likely Efficacy Against Hepatocellular Carcinoma and Markers of Response. Gastroenterology 2019;157:760–76. https://doi.org/10.1053/j.gastro.2019.05.001.
[26] Rebouissou S, Couchy G, Libbrecht L, Balabaud C, Imbeaud S, Auffray C, et al. The beta-catenin pathway is activated in focal nodular hyperplasia but not in cirrhotic FNH-like nodules. J Hepatol 2008;49:61–71. https://doi.org/10.1016/j.jhep.2008.03.013.
[27] Vogelstein B, Papadopoulos N, Velculescu VE, Zhou S, Diaz LA, Kinzler KW. Cancer genome landscapes. Science 2013;339:1546–58. https://doi.org/10.1126/science.1235122.
[28] Castellano E, Downward J. Role of RAS in the regulation of PI 3-kinase. Curr Top Microbiol Immunol 2010;346:143–69. https://doi.org/10.1007/82_2010_56.
[29] Delogu S, Wang C, Cigliano A, Utpatel K, Sini M, Longerich T, et al. SKP2 cooperates with N-Ras or AKT to induce liver tumor development in mice. Oncotarget 2015;6:2222–34. https://doi.org/10.18632/oncotarget.2945.
[30] **Ho C, Wang C**, Mattu S, Destefanis G, Ladu S, Delogu S, et al. AKT (v-akt murine thymoma viral oncogene homolog 1) and N-Ras (neuroblastoma ras viral oncogene homolog) coactivation in the mouse liver promotes rapid carcinogenesis by way of mTOR (mammalian target of rapamycin complex 1), FOXM1 (forkhead box M1)/SKP2, and c-Myc pathways. Hepatology 2012;55:833–45. https://doi.org/10.1002/hep.24736.
[31] Harada N, Oshima H, Katoh M, Tamai Y, Oshima M, Taketo MM. Hepatocarcinogenesis in mice with beta-catenin and Ha-ras gene mutations. Cancer Res 2004;64:48–54. https://doi.org/10.1158/0008-5472.can-03-2123.
[32] Tao J, Zhang R, Singh S, Poddar M, Xu E, Oertel M, et al. Targeting β-catenin in hepatocellular cancers induced by coexpression of mutant β-catenin and K-Ras in mice. Hepatology 2017;65:1581–99. https://doi.org/10.1002/hep.28975.
[33] Satoh S, Daigo Y, Furukawa Y, Kato T, Miwa N, Nishiwaki T, et al. AXIN1 mutations in hepatocellular carcinomas, and growth suppression in cancer cells by virus-mediated transfer of AXIN1. Nat Genet 2000;24:245–50. https://doi.org/10.1038/73448.

[34] Zucman-Rossi J, Benhamouche S, Godard C, Boyault S, Grimber G, Balabaud C, et al. Differential effects of inactivated Axin1 and activated beta-catenin mutations in human hepatocellular carcinomas. Oncogene 2007;26:774–80. https://doi.org/10.1038/sj.onc.1209824.
[35] Qiao Y, Wang J, Karagoz E, Liang B, Song X, Shang R, et al. Axis inhibition protein 1 (Axin1) Deletion-Induced Hepatocarcinogenesis Requires Intact β-Catenin but Not Notch Cascade in Mice. Hepatology 2019;70:2003–17. https://doi.org/10.1002/hep.30556.
[36] Calderaro J, Couchy G, Imbeaud S, Amaddeo G, Letouzé E, Blanc J-F, et al. Histological subtypes of hepatocellular carcinoma are related to gene mutations and molecular tumour classification. J Hepatol 2017;67:727–38. https://doi.org/10.1016/j.jhep.2017.05.014.
[37] Martinez-Quetglas I, Pinyol R, Dauch D, Torrecilla S, Tovar V, Moeini A, et al. IGF2 Is Up-regulated by Epigenetic Mechanisms in Hepatocellular Carcinomas and Is an Actionable Oncogene Product in Experimental Models. Gastroenterology 2016;151:1192–205. https://doi.org/10.1053/j.gastro.2016.09.001.
[38] Lozano A, Souche F-R, Chavey C, Dardalhon V, Ramirez C, Vegna S, et al. Ras/MAPK signalling intensity defines subclonal fitness in a mouse model of hepatocellular carcinoma. Elife 2023;12:e76294. https://doi.org/10.7554/eLife.76294.

Figures Legends

Fig. 1. RSK2 loss-of-function mutations are specific for HCCs and co-occur with Wnt/ß-catenin pathway genetic alterations. (A) Left panel: alteration frequency of *RPS6KA3*/RSK2 in 26 malignancies, right panel: distribution of RSK2 mutations across protein domains and comparison of mutation classes frequency between Coffin-Lowry patients, HCC and non-HCC tumors (Fisher's exact test). Violin plot comparing mutation load between non-HCC tumors mutated or not for RSK2 (Mann-Whitney test). (B) Comparison of *RPS6KA3*/RSK2 mRNA and protein expression between RSK2 mutated and non-mutated HCCs (Mann-Whitney test). (C) Sanger sequencing of *RPS6KA3* on cDNA from 6 mutated HCCs developed in females. (D) Co-occurrence and mutual exclusivity between *RPS6KA3* genomic alterations and 20 other HCC driver genes. (E) Association of RSK2 and AXIN1 inactivation with HCC transcriptomic subgroups (Fisher's exact test). M: "mutated"; NM: "non-mutated", "*": number of tumors analyzed for *TERT* promoter genetic alterations.

Fig. 2. RSK2 inactivation cooperates with AXIN1 inactivation or ß-catenin activation to promote mouse liver carcinogenesis. (A) Upper panel: generation of the three mouse models harboring or not an inactivation of RSK2 combined with either AXIN1 inactivation, or ß-catenin or BRAF activation. Bottom panel: Table comparing liver tumor appearance and their immunohistochemical features, and histological features of the non-tumor liver (NTL) in the different mouse models (Chi-square and Fisher's exact tests were used for categorial variables and Mann-Whitney test for continuous variables). (B) Upper panel: pictures showing liver tumor appearance (circles and arrows) when macroscopically visible in the different mouse genotypes. Bottom panel: representative sections of HES staining and immunostaining of the indicated proteins for each mouse genotype. Asterisks indicate tumors. The same scale bar (200 µm) was applied for all images.

Fig. 3. Transcriptomic profiles of mouse HCCs developed in the different oncogenic cooperation models with RSK2 inactivation mimic those of human HCCs. (A) PCA and hierarchical clustering analysis of 14 mouse HCCs on the 1000 most variable genes (B) Hierarchical clustering of pairwise Pearson correlation coefficients between 196 human HCCs (LICA-FR series) and 14 mouse HCCs from the 6 different mouse genotypes based on an expression signature of 372 one-to-one orthologous genes classifying human HCCs in 6 transcriptomic groups [21]. (C) Heatmap showing the significance of transcriptomic profile association for each mouse tumor with each of the 6 human HCC transcriptomic groups. The main genetic alterations (Alt.) are shown for human and mouse HCCs.

Fig 4. Functional consequences of short-term inactivation of RSK2 and/or AXIN1 in the liver of 6 weeks old mice. (A) Impact of RSK2 and/or AXIN1 loss on the proliferation index, number of oval cells per portal tract and bile duct diameter (Mann-Whitney test). (B) PCA on the top 500 most variable genes between the four mouse genotypes. (C) Venn diagram illustrating the number of unique and shared DEGs for each comparison. (D) GSEA analysis of liver transcriptomic profiles for the four comparisons: (left panel) Heatmap of NES for the two main categories of gene sets significantly enriched in the four comparisons. (right panel) Proportion of each category of gene set with positive and negative NES among the entire significant gene sets for each comparison. *P*-values indicate: on the top, difference between the three genotypes (Chi-square test), on the right difference between positive and negative NES within each genotype (Fisher's exact test).

Fig.5. RSK2 deficient liver cancer cells are dependent on RAS/MAPK signaling activation for their survival. (A) Lentiviral rescue of RSK2 expression in the RSK2 deficient Hep3B HCC cell line carrying a deletion in the *RPS6KA3* gene. (B) Effect of RSK2 rescue in Hep3B cells on ERK phosphorylation, cell survival and sensitivity to inhibitors targeting the RAS-MAPK and PI3K/mTOR signaling pathways assessed either by the GI50 or the AUC after 72h of treatment. A t-test was used for statistical comparisons. MOI: multiplicity of infection

Figure

Click here to access/download;Figure;Figure 1_revised.pdf

Fig. 1

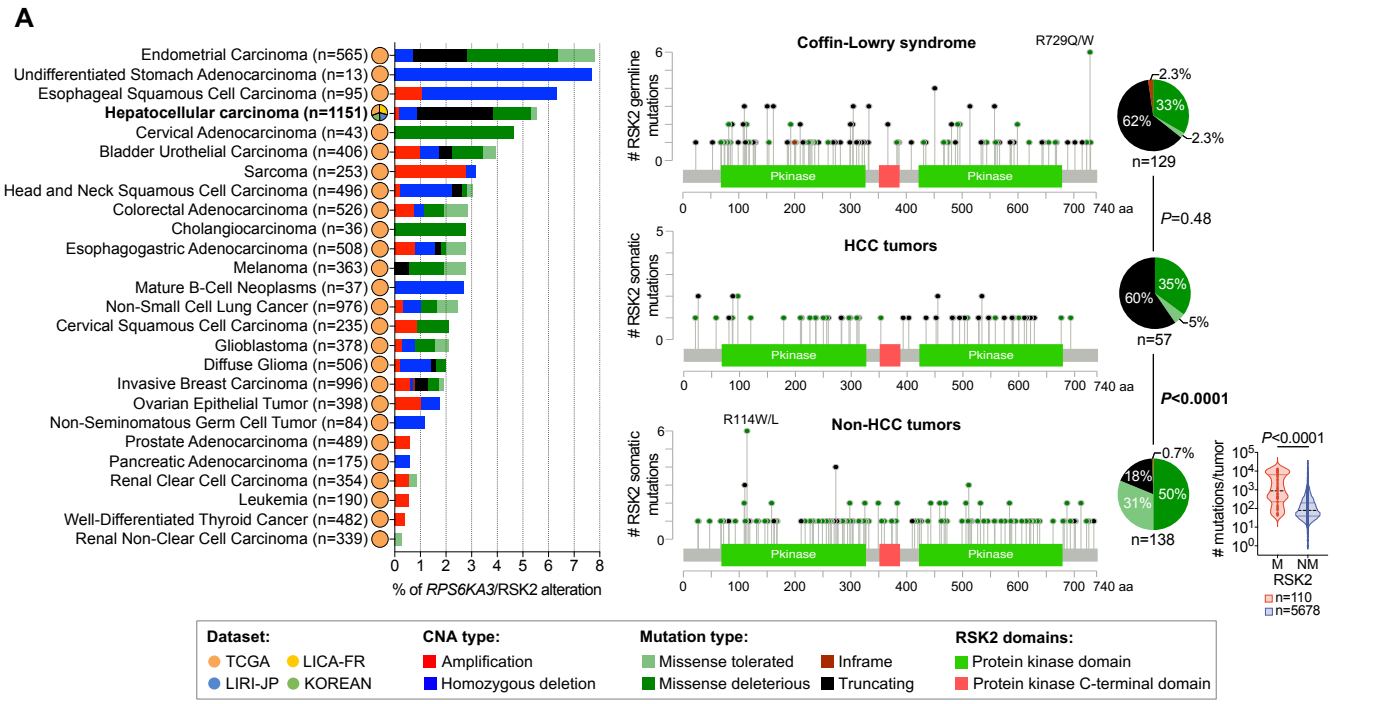

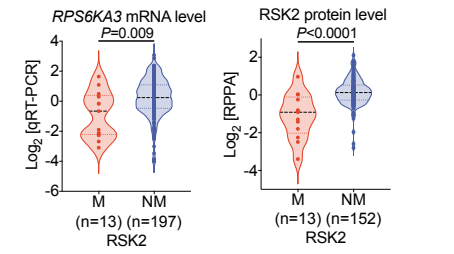

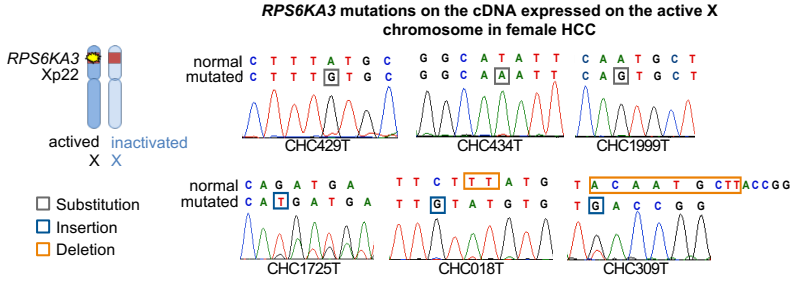

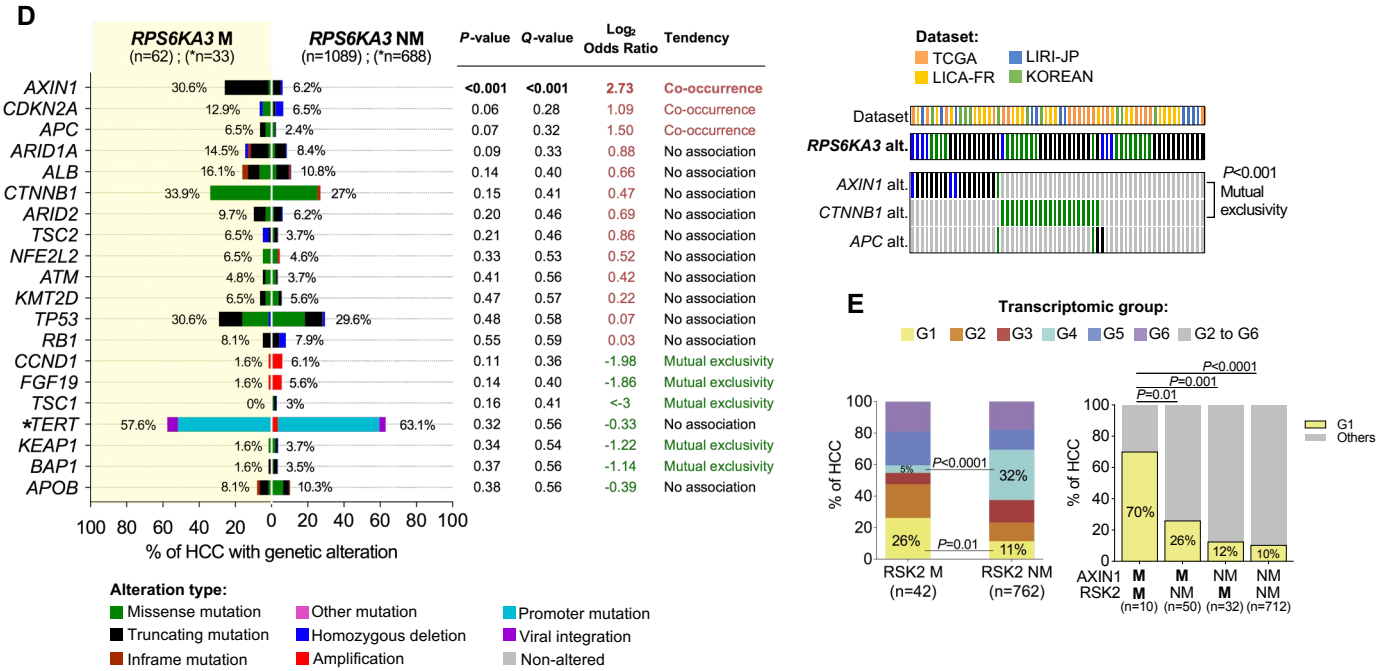

Figure

Click here to access/download;Figure;Figure 2_Revised.pdf

Fig. 2

A

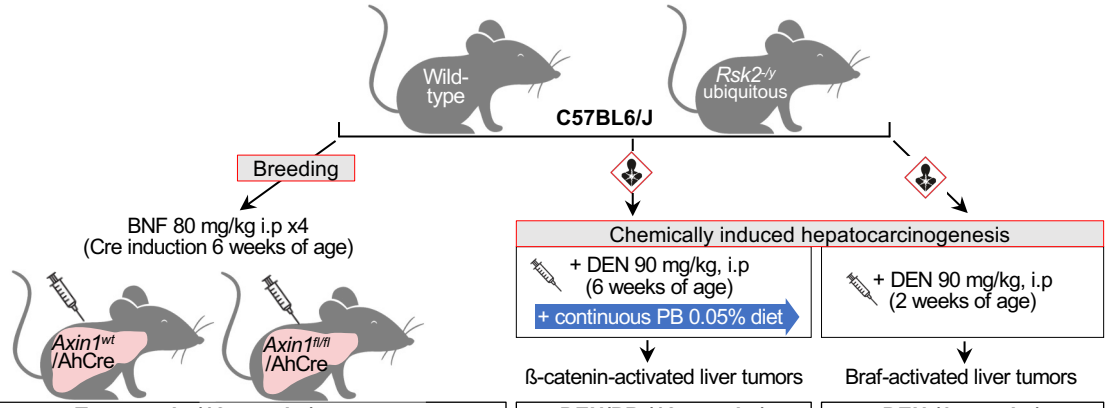

Mouse model	Transgenic (12 months)					DEN/PB (12 months)			DEN (6 months)		
Oncogenic cooperation tested	*Rsk2*^{wt}; *Axin1*^{wt}/AhCre	***Rsk2***$^{-/y}$; *Axin1*^{wt}/AhCre	*Rsk2*^{wt}; *Axin1*$^{fl/fl}$/AhCre	***Rsk2***$^{-/y}$; *Axin1*$^{fl/fl}$/AhCre	*P*-value	*Rsk2*^{wt}; *Ctnnb1*	***Rsk2***$^{-/y}$; *Ctnnb1*	*P*-value	*Rsk2*^{wt}; *Braf*	***Rsk2***$^{-/y}$; *Braf*	*P*-value
# of mice	n=10	n=11	n=12	n=8		n=10	n=8		n=10	n=12	
Tumor frequency	0%	0%	8.3%	62.5%	**0.0003**	50%	100%	**0.036**	80%	75%	1
# of nodules/mouse mean ± SD	0	0	1	5.2 ± 4.9	n.d	4.2 ± 3	4.6 ± 3.6	0.96	3.3 ± 2.9	2.2 ± 1.2	0.59
Total # of nodules analyzed in IHC	0	0	1	26		19	37		25	20	
Ki-67 + cells/nodule mean ± SD	-	-	0%	20.7% ± 13.7	n.d	23.7% ± 11.2	15% ± 10.3	**0.003**	15.8% ± 9.6	7.2% ± 14.1	0.91
GS + nodules	-	-	0%	0%	n.d	62%	76%	0.37	0%	5%	0.44
Nuclear ß-catenin + nodules	-	-	0%	0%	n.d	41%	76%	**0.03**	4%	5%	1
P-ERK + nodules	-	-	0%	19%	n.d	21%	32%	0.53	44%	80%	**0.018**
P-ERK H-score/ nodule mean ± SD	-	-	0	8.2 ± 24.1	n.d	18.7 ± 53.4	7.8 ± 16.4	0.49	27.2 ± 54.3	73.8 ± 97.4	**0.03**
Liver/body weight % mean ± SD	3.8 ± 0.41	4.1 ± 0.37	5.4 ± 0.73	6.2 ± 1.15	**<0.0001**	9.4 ± 9.24	8.7 ± 7.84	0.33	4.4 ± 0.72	4.6 ± 0.45	0.35
Cellular atypia (NTL)	20%	9.1%	100%	87.5%	**<0.0001**	80%	87.5%	1	40%	33.3%	1

B

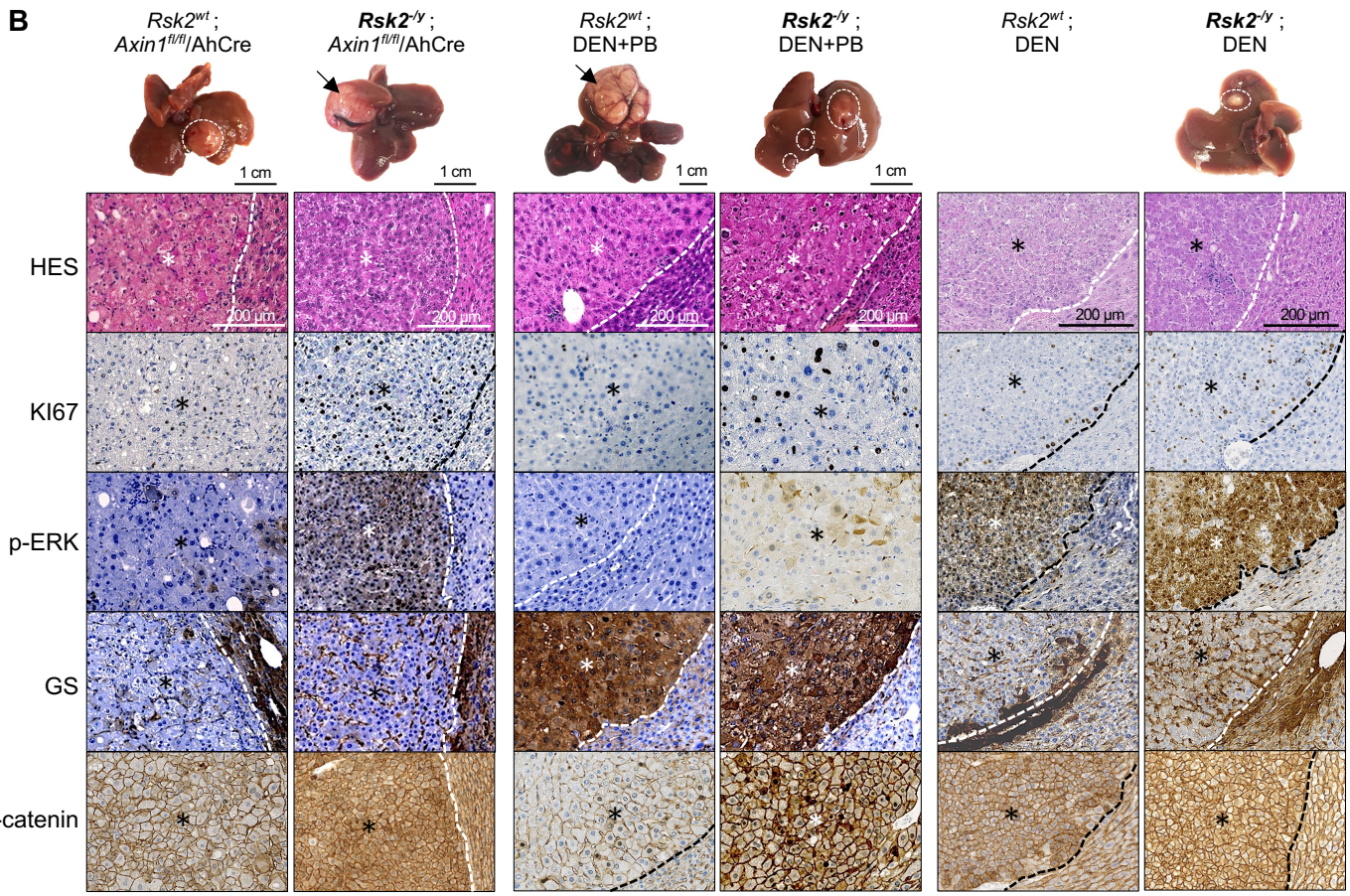

Figure

Click here to access/download;Figure;Figure 3_revised.pdf

Fig. 3

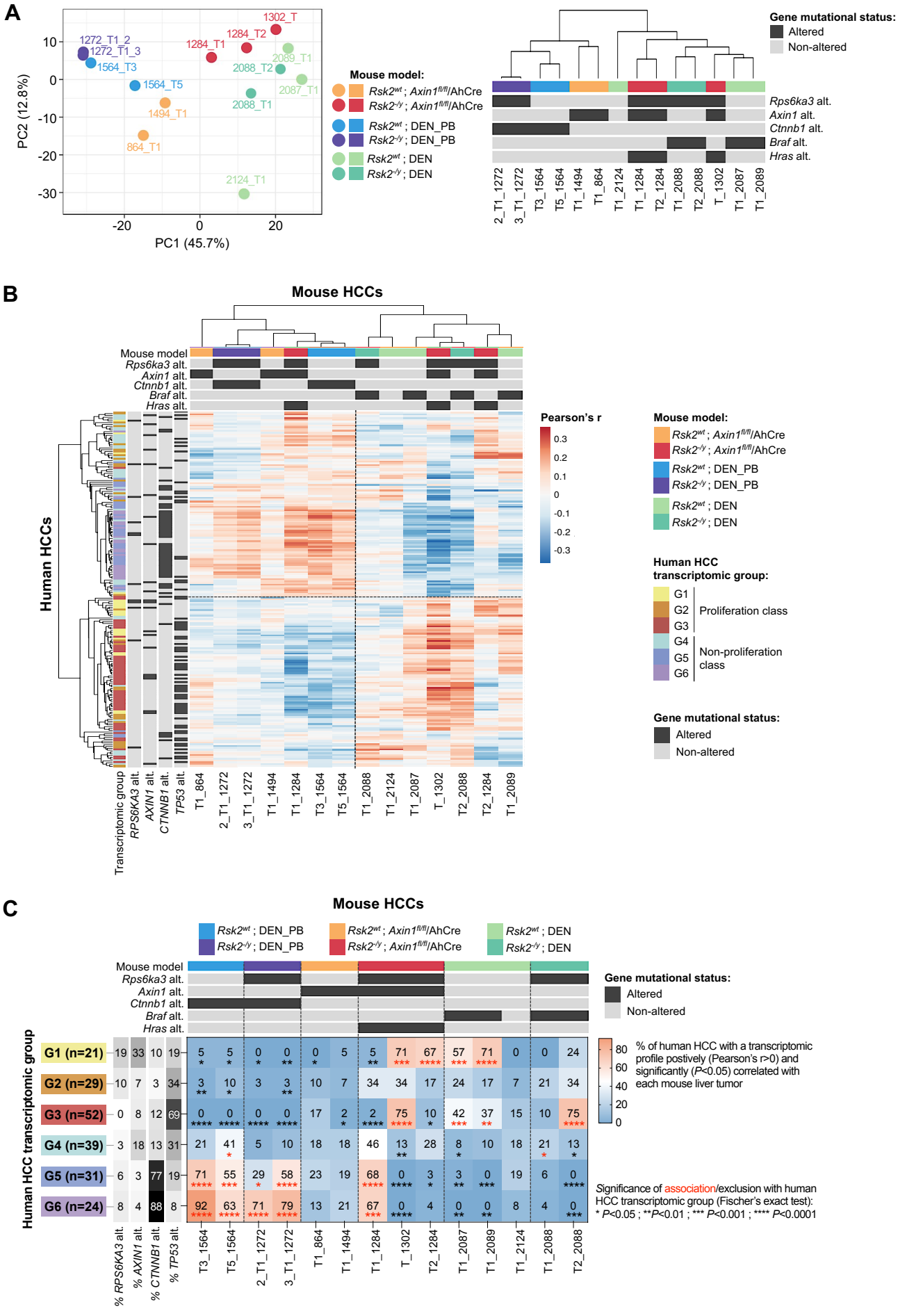

Figure

Click here to access/download;Figure;Figure 4_revised.pdf

Fig. 4

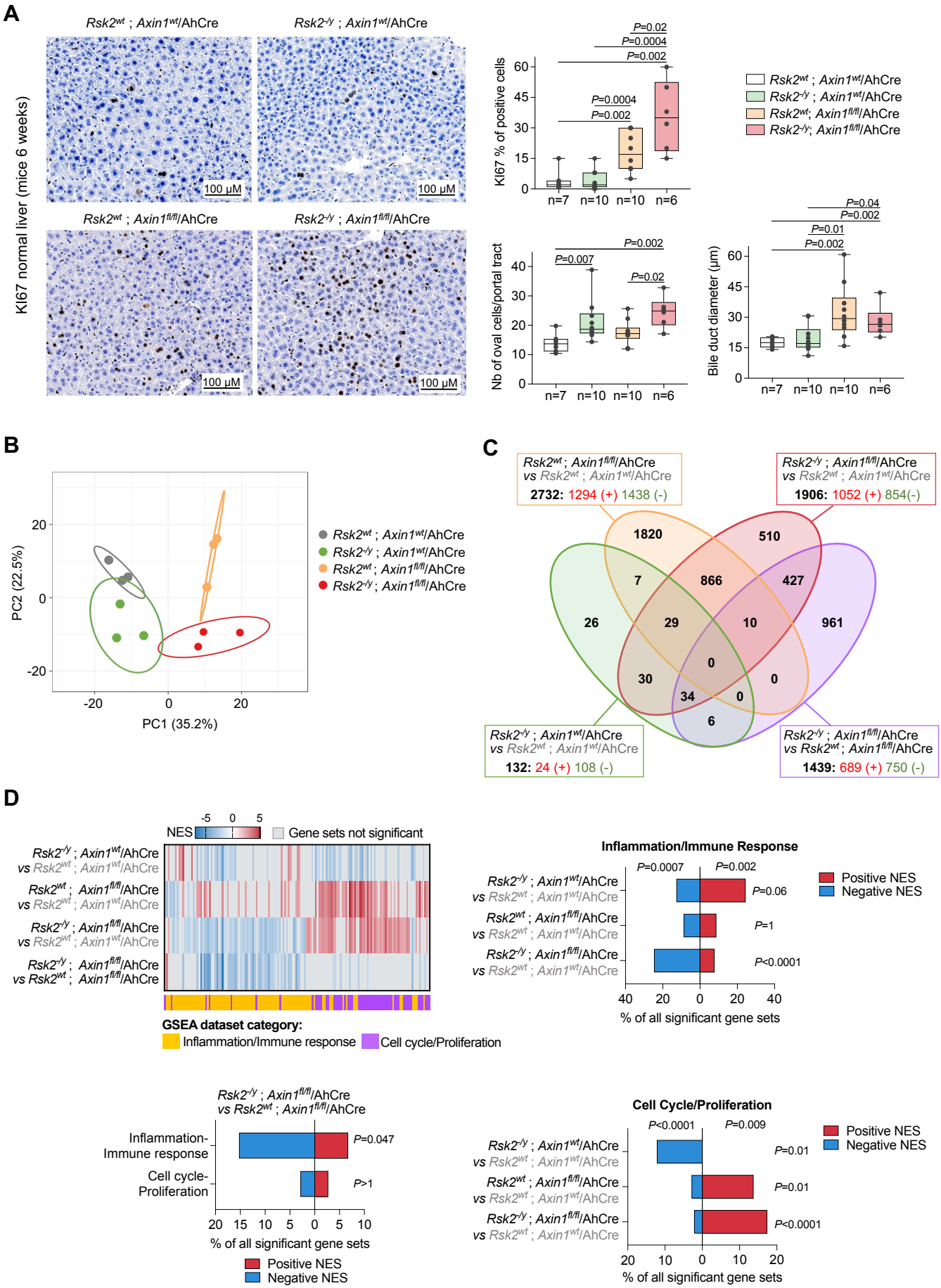

Fig. 5

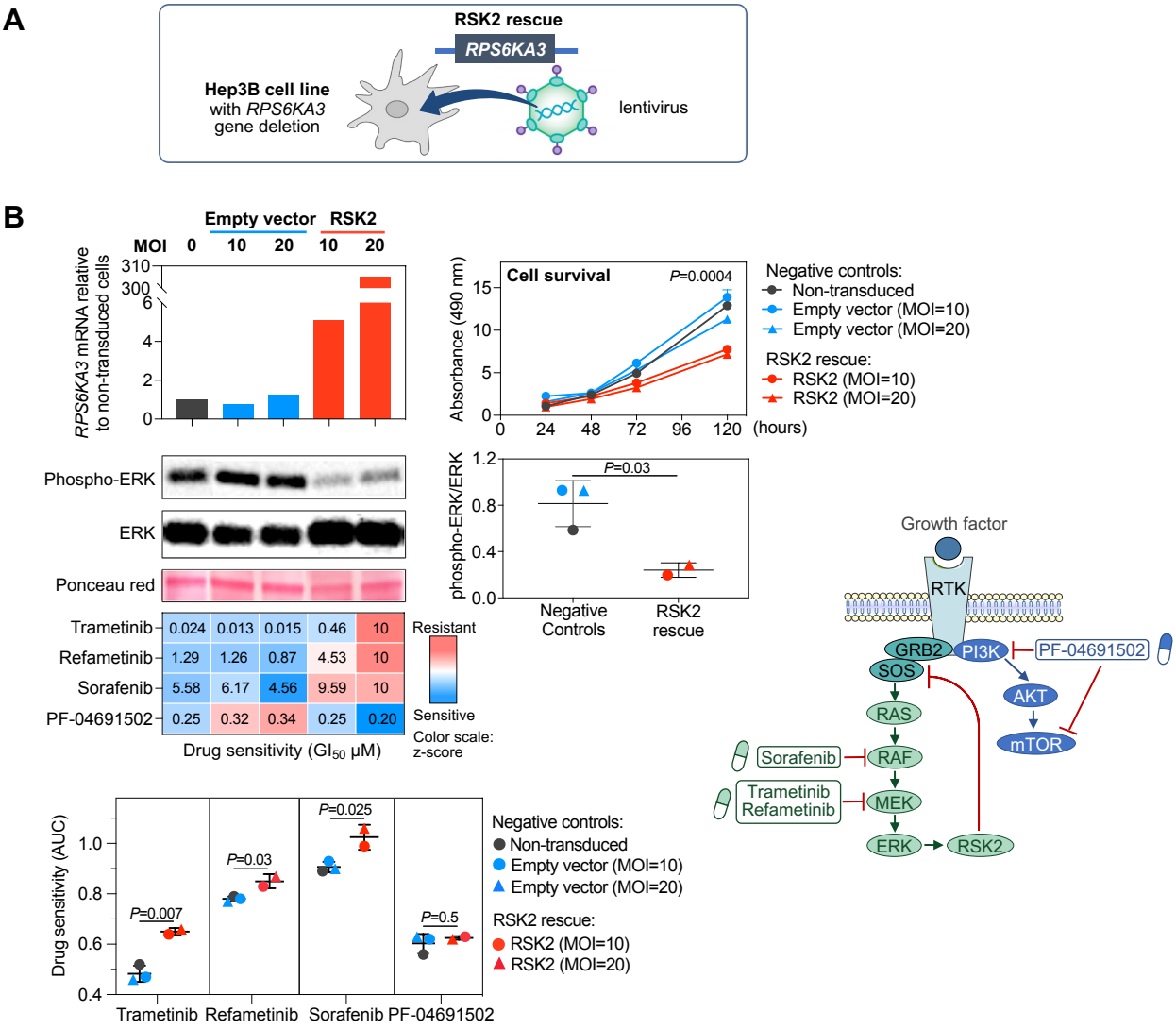

Graphical Abstract

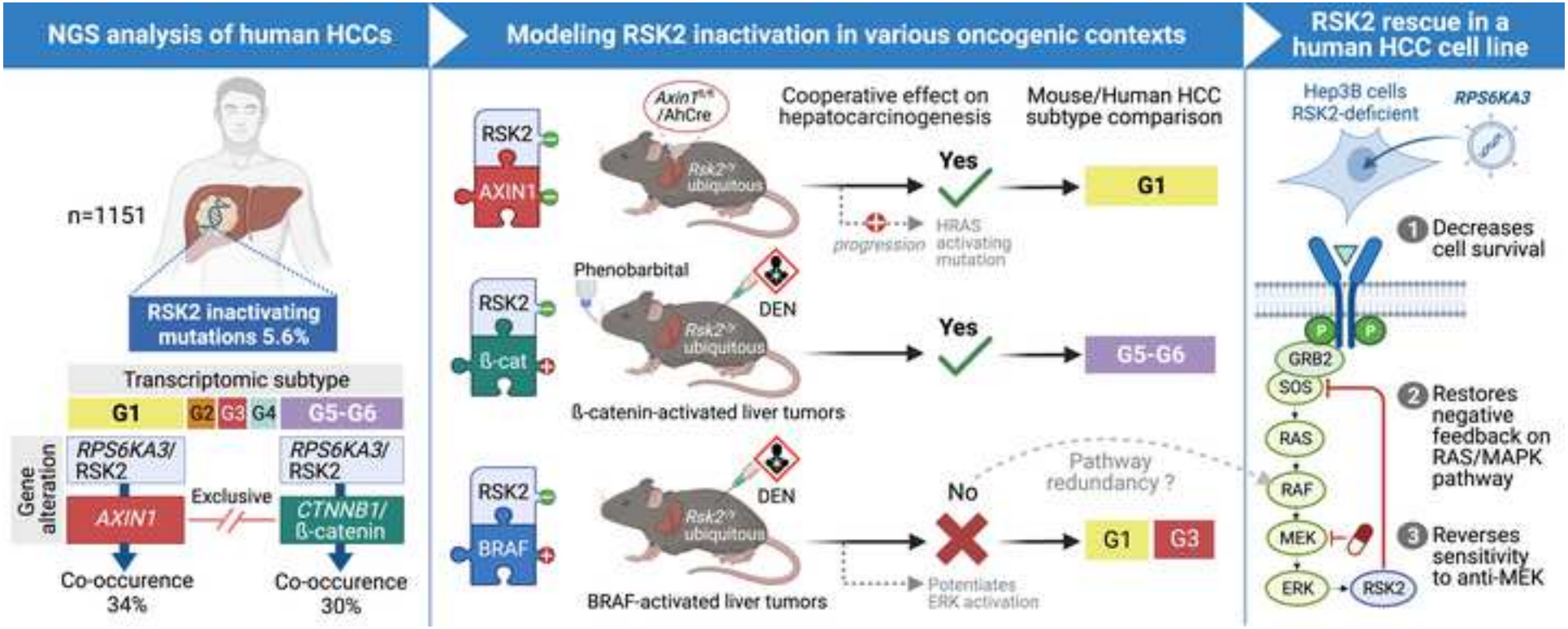

RSK2 inactivation cooperates with AXIN1 inactivation or ß-catenin activation to promote hepatocarcinogenesis

Highlights :

- RSK2 inactivating mutations occur specifically in 5.6% of human HCC
- RSK2 inactivating mutations frequently co-occur with AXIN1 inactivating or ß-catenin activating mutations in human HCC
- In mice, RSK2 inactivation cooperates with AXIN1 inactivation or ß-catenin activation in liver tumor development
- Mouse and human HCC with RSK2/AXIN1 loss or RSK2 loss and ß-catenin activation show similar transcriptomic profiles
- Restoring RSK2 expression in a human HCC cell line decreases cell survival, ERK activity and sensitivity to anti-MEK